American Mineralogist, Volume 78, pages 1275–1285, 1993

REE fractionation between scheelite and apatite in hydrothermal conditions

LOUIS RAIMBAULT*
Laboratoire de Géologie, Ecole des Mines, 158 Cours Fauriel, F-42023 Saint Etienne Cedex 2, France
and Laboratoire Pierre Süe, Groupe des Sciences de la Terre, C.E.N. Saclay, BP no. 2, F-91191 Gif-sur-Yvette Cedex, France

ALAIN BAUMER
Institut de Géodynamique, U.R.A. C.N.R.S., Université de Nice, Parc Valrose, F-06034 Nice Cedex, France

MICHEL DUBRU**
Faculté des Sciences Appliquées, Laboratoire de Minéralogie et Géologie Appliquée, Bt Mercator, Place L. Pasteur 3, B-1348 Louvain la Neuve, Belgium

CONSTANCE BENKERROU
CGGM, Ecole des Mines, 60 Bd Saint Michel, F-75272 Paris Cedex 06, France

VÉRONIQUE CROZE,† ALAIN ZAHM‡
Laboratoire de Géologie, Ecole des Mines, 158 Cours Fauriel, F-42023 Saint Etienne Cedex 2, France

ABSTRACT

The geochemical analysis of hydrothermal apatite and scheelite pairs from various types of W ore deposits (skarns, disseminated scheelite, and quartz veins) provides an insight into REE partitioning between the two minerals. Among the 18 analyzed pairs, only five appear to have grown in equilibrium conditions. Ten other pairs show more or less important departures from equilibrium. The remaining apatite and scheelite pairs have quite different REE patterns, indicating crystallization from different fluids.

Both minerals concentrate REE. The relative behavior of HREE and LREE is quite similar in the two minerals. Scheelite is only slightly more enriched in HREE relative to LREE than apatite, with $K_{\text{ap-sch}}^{\text{La-Yb}} = 0.86 \pm 0.22$. Beside these regularities, some dispersion in the lanthanide content ratios of apatite and scheelite, ranging from 0.6 to 5, may be related to fluid composition. The behavior of Eu can be related to redox conditions, which appear to be more oxidizing in vein associations than in skarn environments. Determination of REE in coexisting scheelite and apatite seems an efficient tool for identification of successive ore-bearing fluids.

INTRODUCTION

The calcium tungstate scheelite ($CaWO_4$) and the calcium fluorophosphate apatite [$Ca_5(PO_4)_3F$] are commonly associated in hydrothermal W ores. However, petrological arguments for their contemporaneity or their precipitation from the same fluid are often ambiguous. Rare earth elements (REE) are easily incorporated in structures of both minerals in substitution for Ca (e.g., Fleischer, 1983, or Roeder et al., 1987, for apatite; Cottrant, 1981, for scheelite). Although such cation exchanges may be used for the characterization of fluids (e.g., Raimbault, 1988), these properties have not been studied extensively. The data suggest similar behavior of both minerals relative to REE, as indicated by a critical examination of natural occurrences.

PREVIOUS WORK

In contrast to the domain of igneous petrology, where the role of apatite in REE geochemistry has been precisely defined during the last decade (e.g., Watson and Green, 1981), information about REE fractionation in hydrothermal minerals is rather scarce. Numerous observations on fluorite veins (Marchand et al., 1976; Grappin et al., 1979; Möller, 1983; Strong et al., 1984; Constantopoulos, 1988; and others) demonstrate the ability of the CaF_2 structure to accommodate trivalent REE cations. Experimental work by Marchand (1976) provides evidence for large partition coefficients for REE in fluorite and fluid, with a partitioning of heavy REE (HREE) into the solid, and an enrichment approximately 15 times greater for Lu than for La. Such large partition coefficients make this mineral an excellent recorder of REE fluid chemistry because precipitation of other phases with low

* Present address: CGGM, Ecole des Mines, 35 rue Saint Honoré, F-77305 Fontainebleau, France.
** Present address: Centre de Recherches de Glaverbel, rue de l'Aurore 2, B-6040 Jumet, Belgium.
† Present address: SPIE ICF, Parc Saint Christophe, Pôle Newton, F-95864 Cergy-Pontoise, France.
‡ Present address: TS-E3X, Rte des Lucioles, Les Algorithmes, F-06370 Sophia-Antipolis, France.

0003–004X/93/1112–1275$02.00

partition coefficients for mineral and fluid does not alter the record of REE chemistry in the fluorite.

In the absence of accurate experimental work for apatite, Raimbault (1985) deduced the enrichment in HREE relative to light REE (LREE) in apatite relative to the mineralizing fluid as follows. Using two independent means, based on separate sets of experimental data (fluorite-fluid by Marchand, 1976, and fluid-melt by Flynn and Burnham, 1978) and of apatite parageneses, it was possible to evaluate concordant values indicating enrichments about four times greater for Lu than for La in apatite, relative to the fluid. These results may be considered as an extension toward low temperatures of the trends observed in magmatic conditions between 1000 and 800 °C by Watson and Green (1981). Starting from an almost symmetrical pattern for the partitioning of REE between apatite and magma, a decrease in temperature favors HREE uptake relative to LREE.

Although there are now some data on REE contents in scheelite (Giuliani et al., 1987; Vinogradova et al., 1982), the response of this mineral to REE composition of fluid is not well known. In order to contribute to solving this problem, we analyzed several apatite and scheelite pairs from various parageneses.

Methods and notation

Methods

Mineral concentrates of both apatite and scheelite crystals were obtained by selective grinding of the initial samples and the use of conventional techniques (heavy liquids and magnetic separation). The final purifications were made by careful hand-picking of minerals under UV light, since scheelite fluoresces blue and our Mn-rich apatite yellow-orange. Analyses were performed by instrumental thermal neutron activation analysis (ITNAA) at Laboratoire Pierre Süe, C.E.N. Saclay (France), using a $4 \cdot 10^{13}$ n/(cm^2·s) thermal neutron flux. Irradiation time of 1–2 h, cooling times of 15 d and 1 month, and counting times of 1–2 and 6–10 h were spent for short-lived (^{140}La, ^{153}Sm, ^{175}Yb, and ^{177}Lu) and long-lived (^{141}Ce, ^{147}Nd, ^{152}Eu, ^{153}Gd, ^{160}Tb) nuclides, respectively. Counting statistics allow an analytical precision of approximately 5% for critical elements (La, Ce, Sm, Eu, Tb, Yb, Lu) in most cases. For some very low HREE concentrations, the precision falls to 10–20%. Most analyzed material weighed around 10 mg, ranging down to <1 mg for some disseminated fine-grained minerals.

Notations

Since we are studying relative REE behavior in two minerals, we are not directly concerned by mineral-fluid partition coefficients. However, scheelite and apatite are not always in contact, and REE exchange is therefore more likely to occur through the fluid phase. The ratio of the concentration of an element i in apatite to that in scheelite is thus not a partition coefficient *sensu stricto* but, as this notation is not ambiguous, we call this ratio an "extended partition coefficient" and denote it as $D^i_{\text{ap-sch}}$. If i represents the lanthanides, we are interested not only in the absolute values of these coefficients, but also in their relative variations. The enrichment factor of element 1 relative to element 2, in mineral X relative to mineral Y is therefore defined as

$$K^{1/2}_{X\text{-}Y} = \frac{[1]_X/[2]_X}{[1]_Y/[2]_Y} = \frac{D^1_{X\text{-}Y}}{D^2_{X\text{-}Y}}$$

where elements 1 and 2 are trace elements replacing a third major element that does not appear here. This expression may be related to a chemical reaction $1_X + 2_Y = 1_Y + 2_X$, but that reaction appears to be fictitious, since it occurs only through the presence of the major element. If elements 1 and 2 are dilute elements, Henry's law applies, and parameter K can be considered to be independent of concentrations of elements 1 or 2.

Let us now comment on the significance of these parameters. If $K^{1/2}_{X\text{-}Y} = 1$, the two minerals X and Y behave identically, whereas if $K^{1/2}_{X\text{-}Y} > 1$, the concentration ratio 1/2 in mineral X is higher than the ratio in mineral Y; that is, the two elements are more fractionated by mineral X than by mineral Y.

In the following, we shall note Ln as a generic term for lanthanide elements. Eu/Eu* stands for the Eu anomaly as the ratio of the measured Eu content to the interpolated value between Sm and Gd (or Tb) in a log scale in chondrite-normalized patterns (also see Appendix 1).

Results and preliminary interpretation

Description of samples containing apatite and scheelite

Eighteen apatite-scheelite pairs were analyzed. Occurrences and corresponding references are summarized in Table 1. As a rule, apatite and scheelite crystals were disseminated throughout the samples, and no mutual relationships could be derived from microscopic observation. We describe briefly the bulk mineral assemblages of the samples.

In the Dajishan garnet muscovite granite (group b in Fig. 1 and Table 1), scheelite and apatite occur as interstitial grains; anhedral apatite is located between feldspar crystals, suggesting a hydrothermal rather than a primary magmatic origin. In the mineralized quartz veins (groups c and d), apatite and scheelite are disseminated in wide muscovite aggregates at the borders of veins; the W-bearing minerals are either scheelite or wolframite and scheelite. In the latter case, wolframite is partly altered to fine-grained scheelite, but it cannot be ascertained whether the larger scheelite crystals analyzed are related to this fine-grained alteration.

In the Costabonne and Coat an Noz skarns (groups e and f), the relationships between scheelite or apatite and garnet suggest that all minerals are cogenetic; moreover, fluid inclusion studies of Costabonne skarns (Guy et al., 1988) reveal identical fluids in the various minerals of the skarn. However, in the analyzed Longobucco skarn

TABLE 1. Nature and origin of samples

Localities	Ref.	Group	Mineral assemblage	Samples
			Granitic environment	
Dajishan, China	1	a	two-mica granite with disseminated apatite and scheelite	307-474
		b	muscovite garnet granite with disseminated anhedral apatite and scheelite	467-23 467-31
			veinlets cutting the muscovite garnet granite	467-20
		c	W-Mo-mineralized feldspar + beryl veins in the contact aureole of granite	467-10 517-21
		d		517-15 517-18
			quartz + wolframite vein	517-1
			Skarn deposits	
Costabonne, France	2	e	scheelite-bearing garnet skarn developed at the expense of biotite granite	8215 8220
Coat an Noz, France		f	quartz + feldspar vein containing scheelite in skarns	Can 66 Can 68
			scheelite-bearing garnet skarn	Can 220 Can 222
Longobucco, Italy	3	g	scheelite-bearing garnet skarn with abundant apatite and sulfides	RO 13
Salau, France	4	h	scheelite + pyrite + chalcopyrite + quartz rock in altered skarn with minor apatite	409.1b
			Quartz wolframite veins in gneisses	
Neuf Jours, France	5	i	quartz + wolframite vein with zoned apatite and white scheelite	NJ S5-6

Note: lower case letters refer to groups in Fig. 1. References: 1 = Raimbault et al., 1986; 2 = Guy, 1980; 3 = Croze, 1989; 4 = Fonteilles et al., 1989; 5 = Raimbault, 1984.

(group g), the primary skarn paragenesis (with garnet and probably scheelite) is replaced by a secondary paragenesis including apatite, fluorite, and sulfides. Similar replacement of a primary skarn paragenesis by a quartz + sulfide assemblage is also present in the analyzed Salau skarn (group h), but in this case both scheelite and apatite seem to be associated with this hydrothermal stage.

In the Neuf Jours vein (group i), apatite crystals are associated with wolframite and strongly zoned from green cores to white rims; scheelite occurs at the center of the quartz veins, but no relationships can be observed.

In all studied occurrences but one, the cogenetic character of scheelite and apatite is far from being demonstrated or ruled out by the conventional microscopic techniques. We therefore used the REE geochemistry of these minerals to investigate these relationships.

Comparison of REE patterns in apatite and scheelite

Analytical results are presented in Tables 2 and 3. Graphical representation of analytical data is given in Figure 1, in which REE patterns of apatite and scheelite are shown in corresponding parts of the diagram. In the eight apatite separates that are related to the Dajishan muscovite-garnet granite (groups b–d in Fig. 1), REE patterns have a quite characteristic shape, convex upward with a strongly negative Eu anomaly. This pattern is related to the granite, the REE pattern of which has the same striking features (Raimbault, unpublished data). Apart from the three scheelite samples 517-1, 517-15, and 517-18 (group d), Dajishan scheelite REE patterns are roughly similar in form to those of the apatite. The large number of samples and the quite specific shape of the patterns exclude any effect due to chance. We must therefore consider that scheelite and apatite retain a similar REE fingerprint with respect to the fluid from which they precipitate. The three exceptions correspond to secondary scheelite, the REE contents of which are inherited from the primary wolframite (Raimbault, unpublished data), allowing an unambiguous answer to one of the questions raised by the petrographic description (see above). These three pairs will not be considered in the following.

The ten other associations display roughly similar REE patterns in scheelite and apatite (Fig. 1), despite various paragenesis (Table 1) and quite different relative REE contents (i.e., REE pattern shapes) in the different pairs, which range from relatively flat patterns, as in Costabonne skarns or in Dajishan two-mica granite, to fractionated patterns, as in Salau skarns. With the exception of the Neuf Jours and Longobucco pairs, the Eu anomaly in apatite is similar to but lower than that in scheelite, leading in some cases to weakly negative anomalies in apatite associated with scheelite with a weakly positive anomaly.

In summary, apart from the three exceptions previously discussed, 15 apatite-scheelite pairs show the following common features: (1) the REE distribution is similar between apatite and scheelite; however, the resulting shape of the pattern varies considerably from one pair to another; (2) the total REE content ratios between apatite and scheelite are variable; and (3) Eu anomalies are comparable in value for apatite and scheelite from the same pair, with a slightly lower anomaly for apatite, despite a very large variation range of >3 log units.

TABLE 2. Analytical results of scheelite

	a	b			c		d		
	307 474	467 23	467 31	467 20	467 10	517 21	517 15	517 18	517 1
La	431	117	78	106	20.1	15.0	3.8	3.1	10.8
Ce	851	582	280	339	62.8	67.1	7.6	8.3	25.9
Nd	827	634	294	361	95	114			
Sm	266	608	209	158	60.4	46.8	4.7	3.7	9.8
Eu	18.5	1.87	2.71	1.75	6.23	4.69	2.40	3.72	3.48
Gd		477	256		136	87	22	20	18
Tb	62.7	46.8	31.3	27.9	23.4	17.8	6.89	6.05	7.61
Yb	142	1.0	0.35	0.70	5.6	4.3	6.3	4.9	2.82
Lu	22.9	<0.15	0.04	0.09	0.80	0.35	0.79	0.52	0.46
Eu/Eu*	0.19	0.012	0.041	0.033	0.24	0.23	0.76	1.44	0.65

Note: lower case letters refer to groups in Fig. 1. Results are given in parts per million.
* INAA analysis by P. Benaben (Ecole des Mines de Saint Etienne).

Similarities and scattering of apatite-scheelite REE ratios

Although the shapes seem to be similar for coexisting apatite and scheelite, which suggests that the two minerals precipitated from the same fluid in each case, the examination of the apatite-scheelite REE patterns provides further refinements. We present these ratios in two figures. In the first case (Fig. 2), five samples from three quite different environments, skarns vs. various granites or feldspar veins, are in perfect agreement with the features defined before. These pairs are characterized by a very weak relative fractionation of REE between scheelite and apatite.

Figure 3 shows more scattered values of apatite-scheelite REE ratios for the remaining pairs. The general tendencies are however to conserve the rather flat shapes already observed above. These departures from ideal patterns do not represent a unique trend, as we observe various behaviors in apatite relative to scheelite. In some cases mid-REE are depleted (at Neuf Jours) or enriched (veinlets in granites at Dajishan) relative to La and Yb. In other cases, LREE (La to Sm in feldspar-bearing veins from Dajishan and at Salau, La to Tb in skarns from Longobucco) are enriched relative to Yb-Lu in apatite relative to scheelite.

At Dajishan, each specific paragenesis is represented by two pairs. The very similar behavior observed in each group indicates that resulting patterns are not due to local effects but reflect a general evolution of the fluid during the first mineralization stage. However, the characteristics of the REE pattern of this fluid remain basically unaltered in scheelite and apatite, as shown by Figure 1, groups b and c. Therefore, the small differences between the two minerals are likely to be due to a delay in the crystallization of scheelite as compared with apatite. Changes in the composition of the fluid leads to a mildly different record of fluid REE pattern in scheelite and apatite, but the delay was short enough to prevent a strong modification of the pattern. REE content of coexisting scheelite and apatite crystals appears therefore as a potential tool for discussing the evolutionary trends in fluid phases.

DISCUSSION

Interpretation of the observed trends

The behavior of REE in aqueous fluids is governed by the stability of the complexes that REE form with various anions. In our samples, ligands that were available in mineralizing fluids certainly include Cl^-, which is the most abundant anion in hydrothermal brines (e.g., Bottrell and Yardley, 1988) and forms complexes with REE at high temperatures (Flynn and Burnham, 1978), and also F^-

TABLE 3. Analytical results of apatite

	a	b			c		d		
	307 474	467 23	467 31	467 20	467 10	517 21	517 15	517 18	517 1
La	175	55.4	89	100	330	191	237	287	190
Ce	663	263	443	466	1134	710	778	959	562
Nd	581	406	494	535	1069	762	689	806	269
Sm	264	332	1115	1084	1074	630	478	570	210
Eu	15.3	1.88	16.5	13.9	24.6	24.3	22.0	16.9	31.8
Gd	374	360	1850		1380	746	494	710	295
Tb	52.5	32.2	214	196	195	110	80.9	121	38.8
Yb	89.7	0.66	1.1	0.8	14.4	6.2	5.9	7.3	7.2
Lu	14.2	0.20	0.10	0.26	1.45	0.55	0.59	0.76	0.80
Eu/Eu*	0.17	0.021	0.043	0.038	0.068	0.12	0.14	0.084	0.45

Note: lower case letters refer to groups in Fig. 1.

TABLE 2.—*Continued*

e		f				g	h	i
8215	8220	Can 66*	Can 68*	Can 220*	Can 222	RO 13	409 1b	NJ S5-6
76	50	24	24	13	19.0	10.0	28.5	3.8
227	170	48	41	20	33.2	25.3	63.7	
126	119							
30.2	19.7	4	4	2	4.8	3.4	4.1	1.1
6.66	9.32	5.6	8.6	2.4	4.77	1.10	5.24	2.79
31	21							
7.15	5.58	0.8	0.8	0.6	0.94	0.34	0.79	0.29
18.5	18.9	5.7	3.5	2.8	2.00	1.2	0.88	0.50
2.72	2.94	1		0.4	0.32	0.27	0.20	0.13
0.60	1.21	4.0	6.2	3.0	2.88	1.17	3.73	6.66

and PO_4^{3-}, which are known as efficient ligands for REE at low temperature (Wood, 1990; Byrne et al., 1991) and were present, as shown by the occurrence of apatite. As no carbonate mineral has been observed, CO_3^{2-} complexing can be considered insignificant. All samples studied therefore correspond to the same set of ligands; their relative availability should however have been different in the different cases, leading to different fluid-mineral partitioning. Nevertheless, we are not studying fluid-mineral exchanges directly, but rather the repartition of REE between two minerals, as well as sorption-coprecipitation reactions involving the breaking of the species for the two minerals, and so the stability constants of the REE complexes can be neglected in a first approximation. (Of course, that is not the case for fluid-mineral exchanges.) However, that quite different ligands (e.g., CO_3^{2-}) result in different partitioning cannot be ignored.

Both apatite and scheelite trap REE. Therefore, precipitation of these minerals leads to a depletion of REE in fluid during crystallization in a closed medium; however, competition effects do not alter the $D^{Ln}_{ap\text{-}sch}$ patterns if the two minerals are strictly synchronous (Appendix 2), the reverse being true if there is some delay in precipitation of one of the two minerals. The result is obviously valid in open systems also. Among the 13 pairs that are constrained by the points outlined above, only five pairs have strictly parallel $D^{Ln}_{ap\text{-}sch}$ patterns (Fig. 2), despite very different environments. The large range of both geological conditions and shapes of the REE patterns rules out the possibility that the regularities observed in Figure 2 are due to chance. Such regularities are therefore an expression of the basic processes that lead to the partitioning of REE between apatite and scheelite. In other words, these ratios result from REE exchanges among apatite, scheelite, and fluid, at or near equilibrium conditions. An evaluation of REE partitioning among scheelite, apatite, and fluorite in experimental conditions, for which contemporaneity of minerals is well established, reinforces this interpretation (Appendix 3). Table 4 gives the measured values of the $D^{Ln}_{ap\text{-}sch}$ parameters, as well as geological setting and estimated fluid parameters for these occurrences. These $D^{Ln}_{ap\text{-}sch}$ values are scattered, as pointed out above, but the identical shape of the five REE ratios results in fairly identical $K^{La\text{-}Yb}_{ap\text{-}sch}$ values. The mean $K^{La\text{-}Yb}_{ap\text{-}sch}$ value is 0.86 ± 0.22, showing that, compared with apatite, scheelite fractionates only slightly more HREE than it does LREE.

In contrast, patterns shown in Figure 3 only mimic the previous figure, leading to scattered $K^{La\text{-}Yb}_{ap\text{-}sch}$ values. Pairs that crystallized from obviously different fluids have already been removed from this discussion; remaining scatter can be interpreted as the result of chemical evolution of one fluid, recorded by apatite and scheelite that are not strictly synchronous. These pairs can therefore be used to evaluate such evolution. We shall discuss briefly here a few examples.

TABLE 3.—*Continued*

e		f				g	h	i	
								NJ S5-6	
8215	8220	Can 66	Can 68	Can 220	Can 222	RO 13	409 1b	core	rim
235	171	141	129	3.4	28.6	9.0	68.2	33.3	66.2
564	497	323	285	9.5	86	24.6	98.6	48.0	108
405	471						28	20.0	54
60.3	84.2	31.7	20.5	0.41	6.9	1.56	6.52	3.20	8.78
6.00	12.2	25.9	24.1	0.52	4.45	1.15	2.76	16.9	32.0
			25.7				6.9		
18.5	17.0	4.97	3.35		1.63	0.28	0.88	0.75	2.33
53.1	84.0	18.9	16.5	0.37	1.5		0.92	4.52	5.83
8.14	13.3	2.92	2.67	0.059	0.35	0.10		1.10	1.03
0.25	0.42	2.55	3.62		1.76	2.20	1.39	14.4	9.55

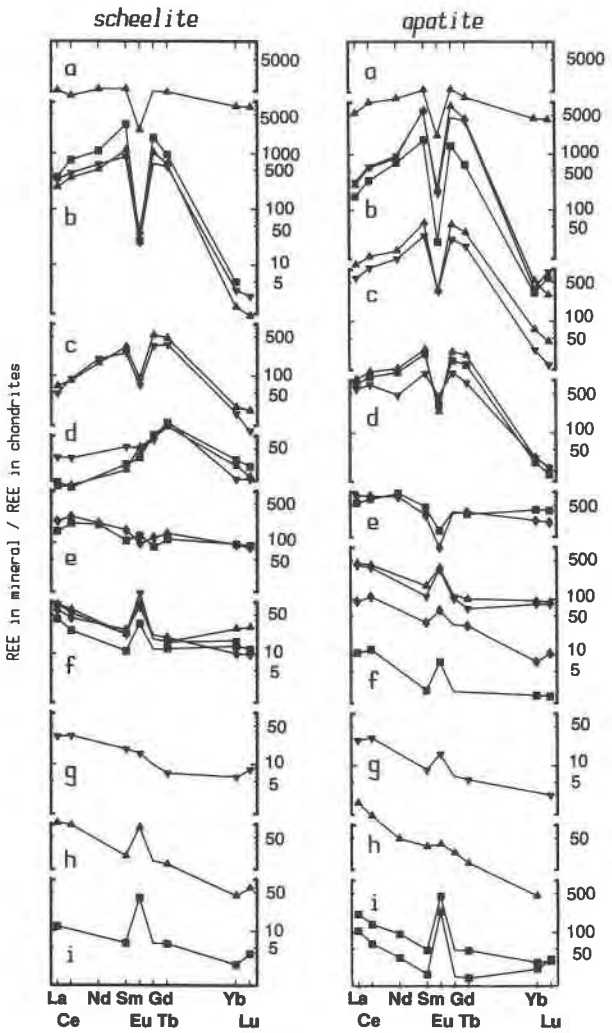

Fig. 1. Chondrite-normalized REE spectra of coexisting scheelite and apatite from various localities and parageneses (see Table 1; chondrite values from Evensen et al., 1978). Samples a–d are from Dajishan, China: (a) disseminated material in two-mica granite, (b) disseminated material and quartz + scheelite veinlets in garnet-muscovite granite, (c) and (d) wolframite + quartz veins; (e) Costabonne, France, garnet skarns; (f) Coat an Noz, France, garnet skarns and feldspar veins cutting the skarn; (g) Longobucco, Italy, garnet skarn; (h) Salau, France, quartz + scheelite + apatite rock in skarns; (i) Neuf Jours, France, quartz + wolframite vein.

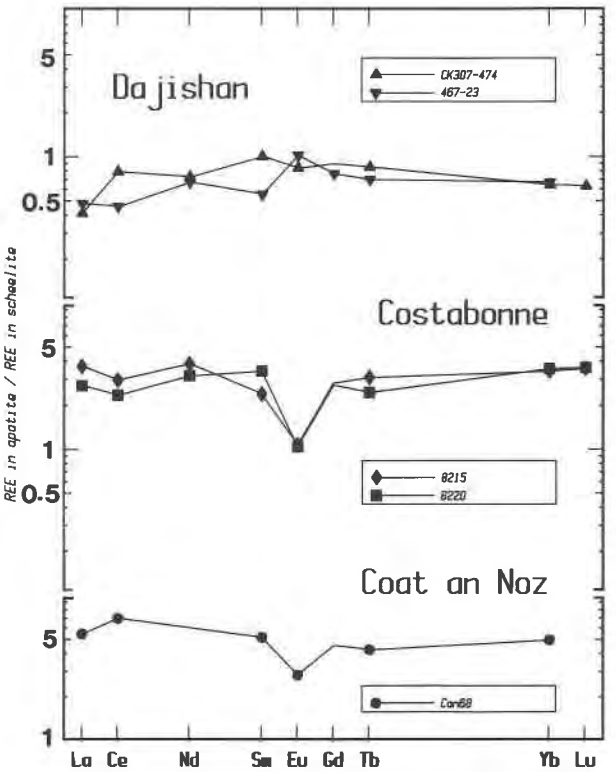

Fig. 2. Plot of REE extended partition coefficients between apatite and scheelite for pairs with identical REE patterns in scheelite and apatite: Dajishan granites (China), Costabonne skarns (France), and Coat an Noz skarns (France).

In the Neuf Jours vein, scheelite is closer to equilibrium with the rims (Fig. 3, solid symbols) than with the cores of apatite crystals (open symbols), the Eu anomaly and the Sm-Tb depletion being weaker in the former case than in the latter. The transition from wolframite toward scheelite as a W-carrying mineral is therefore the result of a continuous evolution of the fluid, the REE contents of which were successively registered by apatite cores, apatite rims, and scheelite. This evolution is probably triggered by mixing with a fluid, the REE pattern of which is characterized by a more usual shape, with a regular slope and without huge positive Eu anomaly. Such a fluid may originate from surrounding gneisses.

At Dajishan, apatite from veinlets in granite is characterized by higher mid-REE contents than scheelite. Knowing that mid-REE are unusually enriched in initial Dajishan fluids, the observed distribution of REE between apatite and scheelite can again be explained by mixing with an externally derived fluid before scheelite precipitates. In feldspar-beryl veins, the most striking feature is a much lower HREE content in scheelite. Since wolframite is known to trap HREE efficiently (Raimbault, 1985), a late crystallization of scheelite as compared with apatite records the HREE depletion due to wolframite crystallization. The few examples presented here show how the analysis of coexisting scheelite and apatite may contribute to qualitative discussions of fluid evolution during ore deposition.

Eu DISTRIBUTION BETWEEN SCHEELITE AND APATITE

Eu may appear in divalent or trivalent forms in natural conditions (Sverjensky, 1984; Bau, 1991), resulting in anomalous behavior as compared with other trivalent REE. Depending on the Eu^{3+}/Eu^{2+} ratio R, and on the differences between the ratios of partition coefficients for Eu^{2+} to Eu^{3+} between phases X and Y relative to the fluid

Table 4. Measured partition coefficients $D^{Ln}_{ap\text{-}sch}$ for natural apatite-scheelite pairs at equilibrium

Localities	Costabonne Skarns		Dajishan Granites		Coat an Noz Feldspar vein
Rocks					
Samples	8215	8220	307-474	467-23	Can 68*
La	3.6	2.7	0.41	0.47	5.4
Ce	2.9	2.3	0.78	0.45	6.9
Nd	3.8	3.1	0.72	0.66	
Sm	2.4	3.4	0.99	0.55	5.1
Eu	1.1	1.0	0.83	1.0	2.8
Gd				0.76	
Tb	3.0	2.4	0.84	0.69	4.2
Yb	3.4	3.5	0.63	0.66	4.9
Lu	3.5	3.6	0.62	<1.3	
$\frac{(La/Yb)_{ap}}{(La/Yb)_{sch}}$	1.08	0.76	0.64	0.72	1.10
Fluid-inclusion data on similar samples**					
T (°C)†			350		330
Salinity (wt% eq. NaCl)			5.5–17.8		4.4–9.5

* Scheelite analysis by P. Benaben (Ecole des Mines).

** References: Costabonne = Guy et al., 1988; Dajishan = Ma and Chen, 1984.

† Average trapping temperatures for pressure estimates of 1.7 (Costabonne) and 1 kbar (Dajishan).

phase ($Ad_{X\text{-}f}$), this anomalous behavior will be more or less reproduced in phases X and Y. Figure 4 illustrates this phenomenon for apatite and scheelite. This diagram is characterized by well-defined straight correlation lines within a specific deposit (Coat an Noz) or part of a deposit (Dajishan, assemblages from granitic environments), or even between similar deposits (Costabonne and Salau skarns). The slopes of these lines are equal to unity; i.e., for each correlation the ratio of the Eu anomaly in apatite A_{ap} to the Eu anomaly in scheelite A_{sch} is constant. The correlated variations of A_{ap} and A_{sch}, either due to variable Eu anomaly A_f in fluid or due to variable redox conditions and hence variable R_f, both lead to straight correlation lines (Appendix 1, Eqs. A2, A3), but a constant ratio $\alpha_{ap\text{-}sch} = A_{ap}/A_{sch}$ is only consistent with variations of the Eu anomaly in the mineralizing fluid under fairly constant redox conditions.

Under such conditions, the ratio $\alpha_{ap\text{-}sch}$ is a function of the oxidation state of Eu in fluid R_f, of the absolute value of the Ad parameters, and of their relative value measured as their ratio $\Omega_{ap\text{-}sch} = Ad_{ap\text{-}f}/Ad_{sch\text{-}f}$ (Appendix 1, Eq. A4). The Ad and Ω parameters are constant at a given temperature, so that a measure of α may provide an estimation of the oxidation state of Eu, provided the Ad parameters and their dependence on temperature were known. If R_f varies from $+\infty$ (trivalent Eu only is present) to 0 (divalent Eu), $\alpha_{ap\text{-}sch}$ varies from 1 to $\Omega_{ap\text{-}sch}$. The position of most points in Figure 4, in the $A_{ap} < A_{sch}$ field, implies that the ratio $Ad_{ap\text{-}f}$ of Eu^{2+} to Eu^{3+} partition coefficients for apatite is lower than the ratio $Ad_{sch\text{-}f}$ for scheelite or, in other terms, scheelite traps Eu^{2+} more efficiently than apatite does. However, the Longobucco and Neuf Jours occurrences plot in the $A_{sch} < A_{ap}$ part of the plan. For Neuf Jours, the evolution brings the points nearer to the $\alpha = 1$ line, and the anomalous location is due to late scheelite crystallization (see above), whereas for Longobucco, there is microscopic evidence for a replacement of scheelite by apatite, and so the two minerals are not at equilibrium.

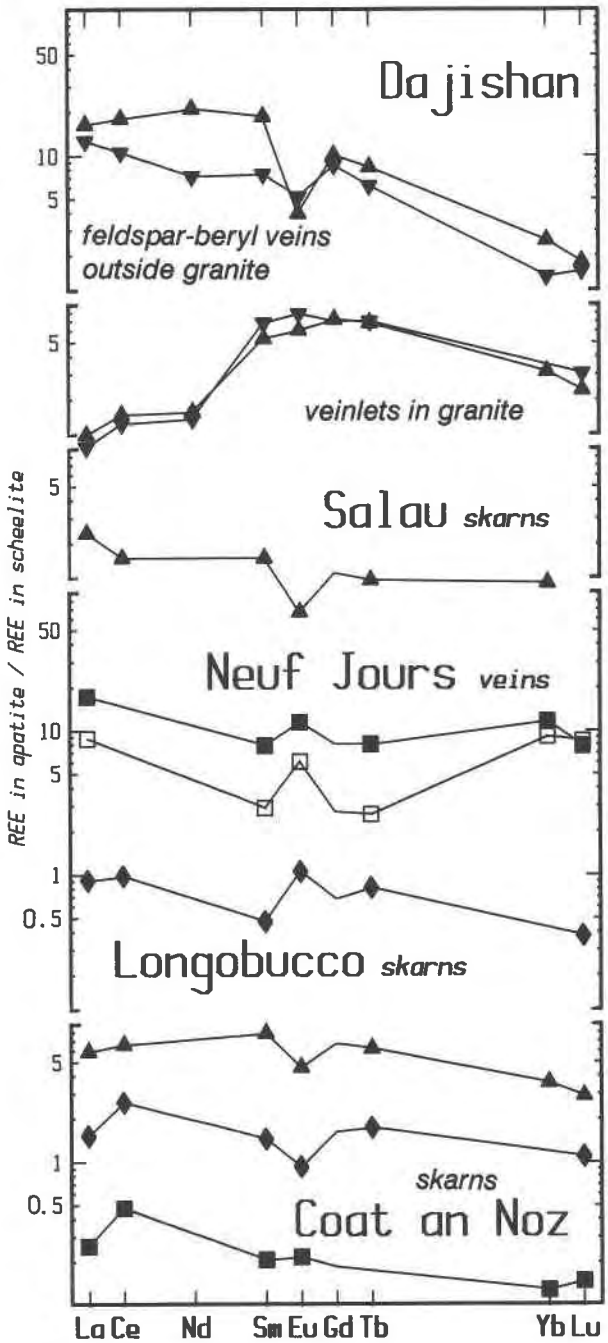

Fig. 3. Plot of REE ratios between apatite and scheelite for pairs with similar REE patterns in scheelite and apatite: vein-type deposits (Dajishan, China; Neuf Jours, France) and skarn-type deposits (Salau and Coat an Noz, France; Longobucco, Italy).

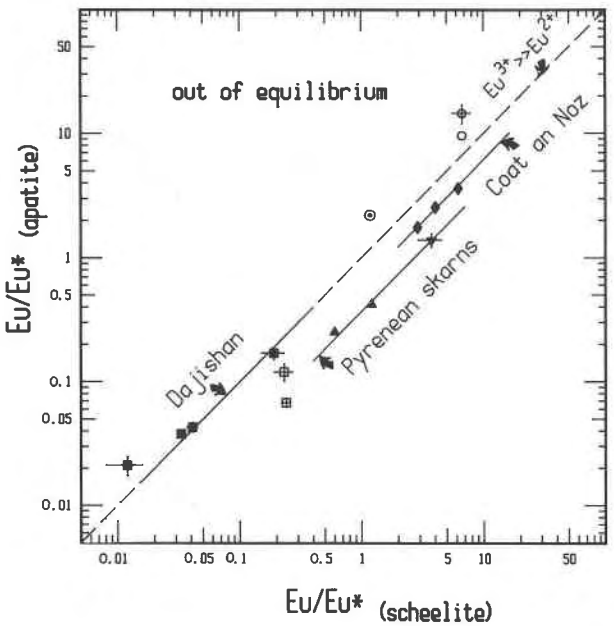

Fig. 4. Eu anomaly (Eu/Eu*; see text) in apatite vs. Eu anomaly in scheelite for coexisting pairs with similar REE patterns. Squares = Dajishan, China; triangles = pyrenean skarns, Salau (inverted triangles) and Costabonne, France; diamonds = Coat an Noz, France; open circles = Neuf Jours, France; circled dot = Longobucco, Italy. The dashed line corresponds to the absence of Eu-anomaly differentiation between the two minerals, indicating the predominance of Eu^{3+}. Above this line, the minerals cannot be considered to be at equilibrium (see text). The lowest Dajishan point corresponds to disseminated material in granite; it is plotted within this zone as a possible result of minor feldspar contamination due to low Eu contents. Some typical analytical uncertainties are shown.

Since formation temperatures for the deposits fall approximately within the same range of 350–500 °C, temperature is not the most important parameter, and the distances of the correlation line from the $A_{sch} = A_{ap}$ line, measured as $\alpha_{ap\text{-}sch}$, are related to local redox conditions, which influence R_f. The occurrence of two independent deposits with very different redox conditions in surrounding rocks (Guy, 1980; Fonteilles et al., 1989) on the correlation line for Pyrenean skarns suggests that this correlation line corresponds to the maximal value of $\alpha_{ap\text{-}sch}$ at these temperatures, providing rough estimation of the $\Omega_{ap\text{-}sch}$ parameter of 0.4–0.35.

Sverjensky (1984) and Bau (1991) have calculated the dependence of f_{O_2} from R_f. For our needs, the corresponding equation can be written $\log f_{O_2} = \log f^0_{O_2} + 4 \log R_f$, where $f^0_{O_2}$ is the value for which $[Eu^{2+}] = [Eu^{3+}]$. This value is dependent on temperature, pH, and activity coefficients (presumed to be constant) of Eu^{2+} and Eu^{3+}. Respective speciation of Eu^{2+} and Eu^{3+} certainly plays an important role in such reactions, but too little is known of their precise roles to be assessed at present. In all occurrences discussed here, the S-bearing phases are sulfides. Therefore, the value of f_{O_2} should correspond to the H_2S domain. Combining this constraint, the value of $\log f^0_{O_2}$ given by Bau for 600 K and pH = 3, and Equation A4, we found that the value for $\log Ad_{sch\text{-}f}$ must be at least about −5, showing that apatite and scheelite trap trivalent Eu much more efficiently than they trap divalent Eu. Calculations by Sverjensky (1984) and Bau (1991) show that at 600 K the $a_{Eu^{3+}}/a_{Eu^{2+}}$ ratio is very small; however, a similar phenomenon has been described for Ce^{4+} in magmatic zircon (Hinton and Upton, 1991), showing that mineral structures can drastically change the existing ratios in fluids.

Table 5. Evaluation of mean REE partition coefficient between apatite and scheelite for equilibrium pairs

Locality	Rock type	$D^{REE}_{ap\text{-}sch}$
Dajishan, China	disseminated in granite	0.71–0.60
Costabonne, France	garnet endoskarn	3.2–2.9
Coat an Noz, France	feldspar veins	5.2

The present estimations of Ad and Ω parameters are not precise enough to deduce a quantitative determination of the oxidation state of Eu and, therefore, of f_{O_2}, from the measure of α parameters. However, Figure 4 provides qualitative results about relative oxidation conditions in the different deposits. In Dajishan granites, most Eu is in the trivalent state in the minerals, and fluids become more reduced at some distance from the granite. Bau (1991) showed that an increase in pH has the same effect that a decrease of f_{O_2} has, and mildly basic pH values are likely in skarn environments. However, differences between Coat an Noz and Pyrenean skarns show that an increase in pH due to a skarn environment cannot account for the bulk effect. Therefore, skarns are characterized by more reducing conditions than vein deposits.

Significance of absolute values of extended partition coefficients

Since the K values of the five equilibrated scheelite-apatite pairs are close to 1, we can define $D^{REE}_{eq\ ap\text{-}sch}$ as the geometrical mean of the individual $D^{Ln}_{ap\text{-}sch}$, excluding Eu, in order to reduce errors due to analytical determination. Despite this processing, $D^{REE}_{eq\ ap\text{-}sch}$ values remain rather scattered, covering almost 1 log unit (Table 5).

Interestingly, there is a correlation between paragenesis and $D^{REE}_{eq\ ap\text{-}sch}$, from lowest values (ca. 0.6) for granite-disseminated minerals, to intermediate values (ca. 3) in skarn deposits, and up to highest values (ca. 5) in vein associations. Observed variations should therefore reflect the chemical influence of the fluid from which apatite and scheelite precipitate.

As shown by the correlations among REE patterns of nearby apatite crystals from the same vein (Knutson et al., 1985), the location of a trace element in a crystal lattice is not strongly modified after its incorporation during crystal growth under hydrothermal conditions. This leads to the following expression of trace element incor-

poration in mineral structure: Ln_{sol} + $PO_{4\,sol}$ + apatite lattice = Ln-bearing apatite.

This equation expresses (1) that the Ln impurity is incorporated into a preexisting crystal structure, and (2) that other elements such as P, F, etc., are needed to close the structure around the Ln ion before the apatite crystal continues to grow. This equation represents an average among all possibilities for introducing Ln into an apatite structure. In this sense, other terms, such as F_{sol}, should be added to the $PO_{4\,sol}$ term, and these terms should be preceded by a coefficient (not necessarily an integer). Therefore, the following discussion should be considered as qualitative. In terms of the chemical equation, we can write the following mass action law:

$$K = \frac{a(\mathrm{Ln})_{ap}}{a(\mathrm{Ln})_{sol} \cdot a(\mathrm{PO_4})_{sol}}$$

where there are of course some missing terms, as, for example, an exponent for $a(PO_4)$, etc., as stressed above. Writing a similar equation for scheelite, we introduce in the expression of $D^{Ln}_{ap\text{-}sch}$ ratios such as $a(PO_4)_{sol}/a(WO_4)_{sol}$. Such ratios are variable from one mineralizing fluid to another, and so we can explain the observed variations of $D^{Ln}_{ap\text{-}sch}$ as well as the correlation between variations and parageneses. Further work could be directed toward the calibration of geochemical tools that would allow an indirect measurement of such ratios.

Conclusions

Careful evaluation of REE partitioning between apatite and scheelite strongly supports the hypothesis that both minerals fractionate HREE relative to LREE in similar quantities, with a slightly lower enrichment of HREE in apatite relative to scheelite by a factor $K^{La\text{-}Yb}_{ap\text{-}sch} = 0.86 \pm 0.22$. No differential behavior can result from differences arising from the more or less closed character of a system if the minerals are strictly synchronous. The study of REE partitioning between coexisting scheelite and apatite appears therefore as a promising tool for discussing equilibrium between the two minerals, as well as for correlating departures from equilibrium with paragenesis or chemical variations in ore-bearing fluid. Comparison of Eu anomalies in the two minerals provides some insight into the oxidation state of Eu and, therefore, into redox conditions of ore deposition. Mean values of $D^{REE}_{ap\text{-}sch}$ are related to mineral parageneses, and their dispersion probably reflects variations of some elemental ratios in mineralizing fluids.

Acknowledgments

We thank B. Guy and Jan Hawkes, who provided helpful comments on the first draft of this paper. The manuscript was also substantially improved by further review by Trevor Green, Gaston Giuliani, Michael Bau, and an anonymous referee. Research was supported by the Commission of European Communities under contract no. MSM040F, by A.T.P. Transferts of the C.N.R.S. under grant no. 1576-AP85, and by A.T.P. Métallogénie-Géochimie under grant no. 8311.

References cited

Bau, M. (1991) Rare-earth element mobility during hydrothermal and metamorphic fluid-rock interaction and the significance of the oxidation state of europium. Chemical Geology, 93, 219–230.

Baumer, A., Caruba, R., and Guy, B. (1985) Apatite and tungsten minerals (scheelite and ferberite): A preliminary study of their association by hydrothermal synthesis. Neues Jahrbuch für Mineralogie Monatshefte, 4, 171–178.

Bottrell, S.H., and Yardley, B.W.D. (1988) The composition of a primary granite-derived ore fluid from S.W. England, determined by fluid inclusion analysis. Geochimica et Cosmochimica Acta, 52, 585–588.

Byrne, R.H., Lee, J.H., and Bingler, L.S. (1991) Rare earth element complexation by PO_4^{3-} ions in aqueous solution. Geochimica et Cosmochimica Acta, 55, 2729–2735.

Constantopoulos, J. (1988) Fluid inclusion and rare earth element geochemistry of fluorite from south-central Idaho. Economic Geology, 83, 626–636.

Cottrant, J.F. (1981) Cristallochimie et géochimie des terres rares dans la scheelite: Application à quelques gisements français. Ph.D. thesis, 97 p. University of Paris-VI, France.

Croze, V. (1989) Etude du skarn à tungstène de Longobucco (Calabre, Italie) dans son environnement granitique: Pétrographie et géochimie. Ph.D. thesis, 252 p. University of Paris-VI, France.

Evensen, N.M., Hamilton, P.J., and O'Nions, R.K. (1978) Rare earth elements abundances in chondritic meteorites. Geochimica et Cosmochimica Acta, 42, 1199–1212.

Fleischer, M. (1983) Distribution of the lanthanides and yttrium in apatites from iron ores and its bearing on the genesis of ores of the Kiruna type. Economic Geology, 78, 1007–1010.

Flynn, R.T., and Burnham, C.W. (1978) An experimental determination of rare-earth partition coefficients between a chloride containing vapor phase and silicate melts. Geochimica et Cosmochimica Acta, 42, 685–701.

Fonteilles, M., Soler, P., Demange, M., Derré, C., Krier-Schellen, A.D., Verkaeren, J., Guy, B., and Zahm, A. (1989) The scheelite skarn deposit of Salau (Ariège, French Pyrénées). Economic Geology, 84, 1172–1209.

Giuliani, G., Cheilletz, A., and Mechiche, M. (1987) Behaviour of REE during thermal metamorphism and hydrothermal infiltration associated with skarn and vein-type tungsten ore bodies in central Morocco. Chemical Geology, 64, 279–294.

Grappin, C., Treuil, M., Yaman, S., and Touray, J.C. (1979) Le spectre des terres rares de la fluorine en tant que marqueur des propriétés du milieu de dépôt et des interactions entre solutions minéralisantes et roches sources: Exemple pris dans le district de la Marche Occidentale (France). Mineralium Deposita, 14, 297–309.

Guy, B. (1980) Etude géologique et pétrologique du gisement de Costabonne. Mémoires du Bureau de Recherches Géologiques et Minières, 99, 237–250.

Guy, B., Fauré, N., Le Loc'h, G., and Varenne, J.L. (1988) Etude microthermométrique des inclusions fluides des skarns à tungstène de Costabonne (Pyrénées, France): Quelques résultats. Comptes Rendus de l'Académie des Sciences de Paris, 307, Série II, 33–38.

Hinton, R.W., and Upton, B.G.J. (1991) The chemistry of zircon: Variations within and between large crystals from syenite and alkali basalt xenoliths. Geochimica et Cosmochimica Acta, 55, 3287–3302.

Knutson, C., Peacor, D.R., and Kelly, W.C. (1985) Luminescence, color, and fission track zoning in apatite crystals of the Panasqueira tin-tungsten deposit, Beira-Baxa, Portugal. American Mineralogist, 70, 829–837.

Ma, X., and Chen, W. (1984) Experimental studies of mineral inclusions from the Dajishan quartz-vein type tungsten deposit with an approach to ore genesis. Bulletin of the Institute of Mineral Deposits, 1, 57–69 (in Chinese).

Marchand, L. (1976) Contribution à l'étude de la distribution des lanthanides dans la fluorine. Ph.D. thesis, 81 p. University of Orléans, France.

Marchand, L., Joseph, D., Touray, J.C., and Treuil, M. (1976) Critères d'analyse géochimique des gisements de fluorine basés sur l'étude de la distribution des lanthanides: Application au gîte de Maine (71-Cordesse, France). Mineralium Deposita, 11, 357–379.

Möller, P. (1983) Lanthanoids as a geochemical probe and problems in lanthanoid geochemistry: Distribution and behaviour of lanthanoids in non-magmatic phases. In S.P. Sinha, Ed., Systematics and the properties of the lanthanides, p. 561–616. Reidel, Dordrecht, The Netherlands.

Raimbault, L. (1984) Géologie, pétrographie et géochimie des granites et minéralisations associées de la région de Meymac (Haute Corrèze, France). Docteur-Ingenieur thesis, 482 p. Ecole des Mines, Paris, France.

——— (1985) Utilisation des spectres de terres rares des minéraux hydrothermaux (apatite, fluorine, scheelite, wolframite) pour la caractérisation des fluides minéralisateurs et l'identification des magmas sources et des processus évolutifs. Bulletin de Minéralogie, 108, 737–744.

——— (1988) The recording of fluid phases through REE contents in hydrothermal minerals, a case study: Apatites from the Meymac tungsten district (French Massif Central). In J. Boissonnas and P. Omenetto, Eds., Mineral deposits within the European Community, p. 152–159. Springer-Verlag, Berlin.

Raimbault, L., Liu, Y., Guo, Q., Zhang, Y., Fonteilles, M., and Burnol, L. (1986) REE geochemistry of fluorites from tungsten mineralization at Dajishan, Jiangxi Province, China. Chinese Journal of Geochemistry, 5, 1–14.

Roeder, P.L., MacArthur, D., Ma, X.P., Palmer, G.R., and Mariano, A.N. (1987) Cathodoluminescence and microprobe study of rare-earth elements in apatite. American Mineralogist, 72, 801–811.

Strong, D.F., Fryer, B.J., and Kerrich, R. (1984) Genesis of the St. Lawrence fluorspar deposits as indicated by fluid inclusion, rare earth element, and isotopic data. Economic Geology, 79, 1142–1158.

Sverjensky, D.A. (1984) Europium redox equilibria in aqueous solution. Earth and Planetary Science Letters, 67, 70–78.

Vinogradova, L.G., Barabanov, V.F., Gordukalov, A.I., and Sukharzhevskij, S.M. (1982) Composition and content of the rare-earth elements in scheelite. Zapiski Vsesoyuznogo Mineralogicheskogo Obshchestva, 111, 98–108 (in Russian).

Watson, E.B., and Green, T.H. (1981) Apatite/liquid partition coefficients for the rare earth elements and strontium. Earth and Planetary Science Letters, 56, 405–421.

Wood, S.A. (1990) The aqueous geochemistry of the rare-earth elements and yttrium. I. Review of available low-temperature data for inorganic complexes and the inorganic REE speciation of natural waters. Chemical Geology, 82, 159–186.

Manuscript received June 13, 1991
Manuscript accepted July 12, 1993

Appendix 1. Eu anomaly in coprecipitating minerals

Assuming as a first approximation that Eu^{2+} and Eu^{3+} act as independent elements, that is, there is no oxidation or reduction reaction of Eu during its incorporation into solid structures, the concentration of Eu in the solid phase X is

$$[Eu]_X = D^{Eu^{2+}}_{X\text{-}f} \cdot [Eu^{2+}]_f + D^{Eu^{3+}}_{X\text{-}f} \cdot [Eu^{3+}]_f.$$

The fictitious element Eu* can be calculated as if all Eu were in the trivalent state, and $D^{Eu^{3+}}_{X\text{-}f}$ and $D^{Eu^{*}}_{X\text{-}f}$ were identical. The Eu anomaly in the solid phase X is given by the equation

$$A_X = [Eu]_X/[Eu^*]_X = A_f(R_f + Ad_{X\text{-}f})/(1 + R_f). \quad (A1)$$

Considering two minerals X and Y that crystallize from fluids with a variable Eu anomaly A_f, with other things being equal (especially redox conditions and therefore R_f), we obtain:

$$A_Y/A_X = (R_f + Ad_{Y\text{-}f})/(R_f + Ad_{X\text{-}f}). \quad (A2)$$

If the two minerals crystallize from the same fluid under variable redox conditions, with A_f constant, the elimination of the variable R_f yields the following equation:

$$A_Y = [A_X(Ad_{Y\text{-}f} - 1) + A_f(Ad_{X\text{-}f} - Ad_{Y\text{-}f})]/(Ad_{X\text{-}f} - 1). \quad (A3)$$

In an A_Y vs. A_X diagram, both Equations A2 and A3 represent straight lines, but, in a bilogarithmic diagram, Equation A2 only leads to a straight line (with a slope equal to 1).

Using the same notations as in the text, Equation A2, which can be used as a means to evaluate the oxidation state of Eu, and therefore the redox conditions in the fluid, can be conveniently written in the form

$$R_f = Ad_{Y-f}(\Omega_{X\text{-}Y} - \alpha_{X\text{-}Y})/(\alpha_{X\text{-}Y} - 1). \quad (A4)$$

Appendix 2. The competition effect between coprecipitating minerals

Analytical methods used here give information that pertains to the bulk compositions of the minerals. However, if crystallization conditions are only reflected by surface equilibrium conditions, that is, internal solid diffusion of the elements is negligible during crystallization, these minerals should bear strong zonations (e.g., Knutson et al., 1985).

In a system in which solid phases are not resorbed from the initial state 0 to the final state 1, the total mass of solid M_s is a strictly increasing function of time and can thus be taken as variable. If two solid phases i and j crystallize simultaneously at proportional rates, i.e., dM_i/dM_s and dM_j/dM_s are proportional, it is possible to choose M_i or M_j as a variable instead of M_s. The bulk solid-fluid partition coefficient is given by

$$D_s = \sum_k (D_k \cdot dM_k/dM_s)$$

and is a function of relative crystal growth rates dM_k/dM_s.

The differential formulation of the Rayleigh's law derived from surface equilibrium conditions can be written $dc/c = (D_s - 1)\cdot dM_f/M_f = (1 - D_s)\cdot dM_s/M_s$. The concentration c in the fluid can be derived from this equation as an implicit function of any one of the parameters M_s, M_i, or M_j, as $c = c_1(M_s) = c_2(M_i) = c_3(M_j)$.

Variations of partition coefficients during crystallization are chiefly controlled by ligand concentrations (e.g., Flynn and Burnham, 1978). Partition coefficients can therefore be written as $D_i \cdot \delta_2(M_i)$, where D_i is a constant and $\delta_1(M_s) = \delta_2(M_i) = \delta_3(M_j)$ accounts for the variations of anions in fluid and is therefore identical for the minerals i and j.

The resulting mean concentration c_i in phase i is

$$c_i = \frac{1}{M_i^1} \cdot D_i \int_0^{M_i^1} \delta_2(M_i) \cdot c_2(M_i)\, dM_i. \quad (A5)$$

The mean concentration c_j in phase j is obtained from Equation A5, written for mineral j by the exchange of M_i for M_j, and thus of c_2 for c_3 and δ_2 for δ_3 in the integral. The resulting extended partition coefficient $D_{i\text{-}j}$ is $D_{i\text{-}j} = c_i/c_j = D_i/D_j$.

Whatever the variations of fluid composition, the ratio of the measured concentrations of trace elements in two minerals that coprecipitate from a fluid can be written as the ratio of their partition coefficients relative to the fluid. Competition effects may influence absolute concentrations in minerals, but not their ratio.

Appendix 3. Partitioning of REE between scheelite and apatite through exchange with fluorite

The exchange of REE between apatite and scheelite usually occurs through a fluid phase. It can however be convenient to consider this exchange through a third solid phase that can be analyzed, whereas the fluid phase cannot. Fluorite is ubiquitous and can therefore be used to confirm the previous results.

In the course of an experimental study of coprecipitation of W minerals and other Ca-bearing phases (Baumer et al., 1985), we studied the coprecipitation of fluorite and scheelite from a REE (La, Sm, Gd, Lu) doped chloride brine. Experimental conditions were T = 600 °C, P = 1 kbar, a duration of 72 h, and an initial Cl molality of m_{Cl} = 3.23. The concentration ratio of fluorite to scheelite is determined by ITNAA and directly calculated from γ activity measurements to minimize analytical uncertainties. The resulting $D^{Ln}_{f\text{-}sch}$, 4.01 ± 0.32 (La), 3.46 ± 0.24 (Sm), 4.19 ± 0.41 (Gd), and 8.73 ± 0.42 (Lu), can be combined with $D^{Ln}_{f\text{-}ap}$ values given by Raimbault (1985) to yield a $K^{La/Yb}_{ap\text{-}sch}$ = 0.76. This value, close to the previously determined value of 0.86, provides an additional confirmation of the nearly identical behavior of REE in scheelite and apatite.